Computational Modeling to Study the Treatment of Cardiac Arrhythmias using Radiofrequency Ablation

A. González-Suárez*[1], M. Trujillo[1], J. Koruth[2], A. d'Avila[2], and E. Berjano[1]
[1]Universitat Politècnica de València, Spain, and [2] Helmsley Cardiac Electrophysiology Center, Mt SinaiMedicalCenter and School of Medicine, USA
* Biomedical Synergy, Electronic Engineering Department (Building 7F); Universitat Politècnica de València; Camino de Vera, 46022 Valencia, Spain; angonsua@eln.upv.es

Abstract: Previous studies proposed using bipolar radiofrequency ablation across two catheters placed on opposing surfaces of the ventricular wall to create transmural lesions[1,2]. 2D and 3D models were built and solved numerically using the Finite Element Method (FEM) with COMSOL Multiphysics software. With these models, it was possible to study the temperature distribution and lesion geometry, to compare the potential of two ways of applying electrical currents (bipolar mode, BM, vs. sequential unipolar, SUM) and to investigate the effect of other factors such as the ventricular wall thicknesses and catheter misalignment have never been studied in detail. Our results suggest that BM is in general more effective than SUM in achieving transmurality through the ventricular wall. These results could improve the safety and performance of these procedures.

Keywords: bipolar ablation, cooled electrode, radiofrequency ablation, ventricular ablation.

1. Introduction

Successful radiofrequency ablation (RFA) of ventricular tachycardia (VT) originating from sites in the left ventricle such as the inter-ventricular septum (IVS) is often limited by the presence of deep intramural circuits. The creation of deep or even transmural ablation lesions is therefore warranted, but this cannot always be achieved with 'unipolar RF'. Recent experimental studies have shown that using two catheters placed on opposing surfaces of the IVS[1,2] to deliver RF in the bipolar mode (as opposed to sequential unipolar ablation) allows deeper lesions to be created[1,2] and therefore indicate that BM could be more effective at eliminating VTs in deep intramural sites within the left ventricular free wall or the inter-ventricular septum. However, the effects of different wall thicknesses, catheter alignment and impedance variation (as in the case of endocardium-epicardium bipolar RF) on the efficacy of the transmurality and lesion geometry achieved with bipolar ablation have never been studied in detail. Furthermore, BM and SUM have previously been compared in ablations of the ventricular free wall (VFW), but not for an endocardium–epicardium approach[3]. Although a recent study[4] did consider this approach, the effects of the above mentioned-factors were not included.

Our aim in this study was to assess the thermal lesions created in the ventricular wall, in particular the degree of transmurality in a comparison of bipolar and sequential unipolar RF. Two and three-dimensional RFA numerical models were therefore developed and computer simulations were conducted to investigate temperature distribution and lesion geometry during RFA of IVS (endocardium–endocardium approach) and VFW (endocardium–epicardium approach). The effect of BM and SUM were evaluated in both scenarios.

2. Methods

2.1 Governing equations

Numerical models were based on a coupled electric-thermal problem, which was solved numerically using the Finite Element Method (FEM) with COMSOL Multiphysics software (COMSOL, Burlington MA, USA). The governing equation for the thermal problem was the Bioheat Equation (1):

$$\rho \cdot c \cdot \frac{\partial T}{\partial t} = \nabla(k \nabla T) + q + Q_p + Q_m \qquad (1)$$

where T is temperature, t is time, k is thermal conductivity, ρ is density and c is specific heat. The term Q_p corresponds with the heat loss caused by blood perfusion; and Q_m models the metabolic heat generation. This last term is always ignored in RF ablation modeling since it has been shown to be insignificant. It has also been shown that the Q_p term can be ignored in

the case of cardiac ablation. Finally, the term q is the heat source from RF power (Joule loss) which is given by $q = \sigma \cdot |E|^2$, where $|E|$ is the magnitude of the vector electric field (V/m) and σ is the electrical conductivity (S/m). The value of this vector is calculated from $\vec{E} = -\nabla\Phi$, where Φ is the voltage (V). The voltage is obtained by solving Laplace's equation, which is the governing equation of the electrical problem:

$$\nabla \cdot \sigma \nabla\Phi = 0 \qquad (2)$$

At the RF frequencies (≈500 kHz) used in RF heating and for the geometric area of interest, the biological medium can be considered almost totally resistive. A quasi-static approach is therefore possible to solve the electrical problem[5].

Tissue vaporization was modeled by using the enthalpy method[6]. This was performed by modifying Equation (1) and incorporating the phase change as follows:

$$\frac{\partial(\rho h)}{\partial t} = \nabla(k\nabla T) + q + Q_p + Q_m \qquad (3)$$

where h was the enthalpy. For biological tissues, the enthalpy is related to the tissue temperature:

$$\rho h = \begin{cases} \rho_l c_l T & 0 < T \le 99\,^{\circ}C \\ \rho h(99) + h_{fg} C \dfrac{(T-99)}{(100-99)} & 99 < T \le 100\,^{\circ}C \\ \rho h(100) + \rho_g c_g (T-100) & T > 100\,^{\circ}C \end{cases} \qquad (4)$$

where ρ_i and c_i were tissue density and specific heat of liquid tissue (i=l) and the post-phase-change tissue (i=g), respectively; h_{fg} was the latent heat and C the tissue water content. We considered a value of latent heat of $2.162 \cdot 10^9$ J/m^3, which corresponds to the product of the water vaporization latent heat and the water density at 100ºC, and a tissue water content of 0.75 inside the cardiac tissue.

2.2 Numerical models

The models considered two internally cooled catheter tip electrodes (7Fr diameter, 4 mm catheter tip), similar to those used in cardiac RFA.[3] Figure 1 shows the proposed general geometry of the models for the case of IVS ablation, i.e. endocavitary blood surrounding both electrodes placed perpendicular to the septal surfaces (endocardium–endocardium approach). The VFW ablation model was implemented with the assumption that the epicardial catheter was surrounded by pericardial fluid (endocardium–epicardium approach). Since the region under study has axial symmetry, a two-dimensional model could be used. The ventricle dimensions X and Z were estimated by means of a convergence test in order to avoid boundary effects. Another convergence test was performed to obtain adequate spatial (i.e. minimum meshing size) and temporal resolution[7]. We also built three-dimensional models which were used to represent a scenario in which the two electrodes were not aligned exactly opposite each other. These 3D models also allowed for simulation of parallel placement of the epicardial catheter tip (as opposed to perpendicular) to the epicardium during VFW ablation.

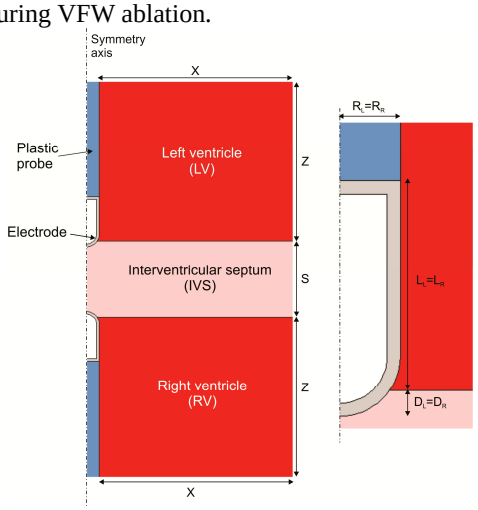

Figure 1. Numerical model considered for IVS. S: septum thickness, electrode radius: R_L=R_R= 1.155 mm (7Fr), electrode lengths: L_L = L_R = 3.5 mm (0.25 mm thickness wall), and insertion depth: D_L= D_R= 0.5 mm.

The thermal and electrical characteristics of plastic, metal, cardiac tissue and blood were obtained from previous modeling studies.[8,9] The electrical and thermal conductivity were temperature-dependent functions and we used piecewise functions. Analytically, the piecewise functions were defined using the Heaviside function, which in COMSOL was substituted by the smoothed function[10] *flc2hs*. For the electrical conductivity (σ) we considered an exponential growth[8] of 1.5%/ºC up to 100ºC and then it decreased 4 orders for five degrees. The thermal conductivity (k) grew linearly 0.001195 K^{-1} up to 100ºC, after which temperature k was kept constant.

To model BM, an electrical isolation boundary condition was set at the model limits. A voltage drop of 40 V was applied between the

electrodes throughout the total ablation time of 120 s, so that the electrical currents were always forced to flow between both electrodes. In contrast, a constant zero voltage was set at the model limits (mimicking the electrical performance of the dispersive electrode) when modeling SUM. In addition, one of the active electrodes was set at 40 V and the other was electrically isolated for the first 60 s, following which the electrical conditions were reversed for the last 60 s (sequential mode with electrical currents forced to flow between the ablation and dispersive electrodes). Both the initial temperature and the temperature of the surface away from the active electrode were assumed to be 37ºC. The endocardium−epicardium approach was modeled by replacing the circulating blood with pericardial fluid on the epicardial side. Due to the lack of information on the electrical and thermal characteristics of this fluid we assumed the characteristics of saline as an approximation. We also conducted computer simulations in which the pericardial fluid was replaced with air. Although as a rule the epicardial space does not contain any air, during epicardial puncture and instrumentation, small amounts of air may accumulate around the ablation catheter. These simulations represent a worst case scenario, with air around the ablating electrode only.

Different thermal convection coefficients were considered in the endocardium–blood (3,636 W/m^{2}K), electrode–blood (708 W/m^{2}K)[9] and epicardium–air/pericardial fluid (20 W/m^{2}K) interfaces. The internal cooling of the electrode was modeled with a coolant temperature of 21ºC (room temperature) and a thermal convection coefficient of 10,629 W/m^{2}K, estimated by using the theoretical calculation forced convection inside a tube.[7] Ventricular wall thickness (IVS or VFW) was varied between 5 to 15 mm. The thermal lesions were assessed using the Arrhenius damage model with parameters from Jacques and Gaeeni,[11] i.e. damage to tissue due to heating was calculated as a function of both temperature rise and exposure time.

3. Results

We obtained a value of X = Z = 40 mm, a grid size of 0.2 mm in the electrode–tissue interface and a step time of 0.05 s from the convergence tests. Tissue temperature did not reach more than 111ºC in any of the simulations and the temperature in the electrode was always lower than 50ºC.

2.3 Interventricular septum ablation (IVS)

a) Bipolar mode (BM): The temperature distributions in the tissue after RFA using bipolar mode across the IVS are shown in Fig. 2. The solid black line indicates the thermal damage borderline and therefore outlines the lesion. Although the lesions were always transmural and symmetrical when the septal wall was between 5 and 15 mm thick, the lesion geometry differed slightly with thickness. When this was ≤ 10 mm, the maximum lesion width occurred in the middle of the septum (Fig. 2a). However, at ≥ 12.5 mm the lesion had an hourglass shape, with the minimum width at the middle of the septum (Fig. 2b).

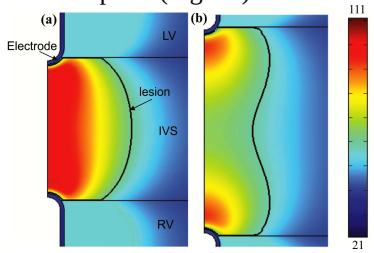

Figure 1. Temperature distribution in the tissue after 120 s of bipolar RFA across the IVS for septal thickness: (a) 10 mm and (b) 15 mm. Scale in ºC.

b) Sequential unipolar mode (SUM): The results of SUM differed significantly from those obtained from the BM. Figure 3 displays the temperature distributions in the tissue after RFA for different septal thicknesses.

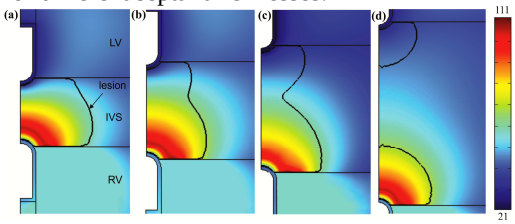

Figure 3. Temperature distributions in tissue after 120 s of sequential unipolar RFA (catheter on top was activated firstly) across the IVS; septum thickness of (a) 5 mm (b) 7.5 mm (c) 10 mm and (d) 15 mm.

The most significant finding from the SUM was that it was not possible to create transmural lesions in septa over ≥12.5 mm (Fig. 3d), nor was it possible to achieve symmetrical lesions. Even when the septal thickness was 15 mm,

when one would expect two identical lesions to be created independently due to the large distance between electrodes (Fig. 3d), the lesions remained asymmetrical. In fact, lesion depth around the first activated electrode during sequential ablation was 3.7 mm, as compared to 5.0 mm on the other side in which the electrode was activated second. The lesions were found to be in general wider around the second activated electrode (Fig. 3a-c).

When the superiority of BM over SUM in creating transmural lesions in the IVS had been suggested by the results, we then assessed the effect of progressive misalignment between the electrodes on lesion dimension and contiguity, for which we used a three-dimensional model due to the lack of axial symmetry in this situation. Figure 4 shows the tissue temperature using BM across the IVS (10 mm septum thickness) by varying the misalignment between the electrodes from 0 (no misalignment) to 10 mm (maximum misalignment). The lesions were seen to become longer as the misalignment increased and the lesion shape became more hourglass-like (see Fig. 4e). Even under these conditions, the lesions were transmural, i.e. there was thermal damage in the center of the tissue.

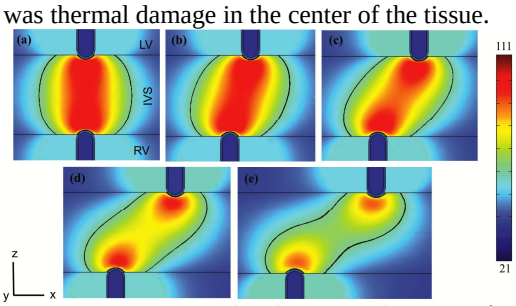

Figure 4. Temperature distributions in the tissue after 120 s of bipolar RFA across the IVS (10 mm septum thickness) with purposeful misalignment by (a) 0 mm (b) 2.5 mm (c) 5 mm (d) 7.5 mm and (e) 10 mm.

2.4 Ventricular free wall ablation (VFW)

a) Bipolar mode (BM): Figure 5 shows temperature distributions in the tissue after RFA across VFW. Two different situations were analyzed: a) epicardial catheter tip surrounded by air and b) by pericardial fluid. The most important finding was the lack of thermal lesions on the endocardial side when air was considered to surround the epicardial catheter tip (Fig. 5a). In this scenario, the lesion on the epicardium was never transmural and had a depth and width of approximately 3 mm and 6 mm. On the contrary, when pericardial fluid was considered to surround the epicardial catheter tip, the lesions were transmural and symmetrical for thicknesses up to 15 mm (Fig. 5b).

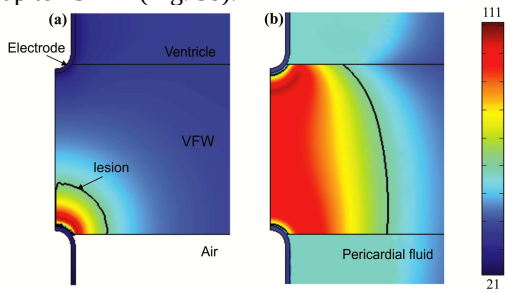

Figure 5. Temperature distributions in the tissue after 120 s of bipolar RFA across the VFW (10 mm thickness) with the epicardial catheter surrounded by (a) air and (b) pericardial fluid.

Figure 6 shows the temperature distribution and lesion shape for the scenario in which the catheter tip is completely covered by pericardial fluid. It also displays the effects of the perpendicular and parallel orientation of the epicardial catheter tip. The temperature distributions in both situations were almost identical, which indicates that the orientation of the catheter does not have a significant effect on lesion geometry.

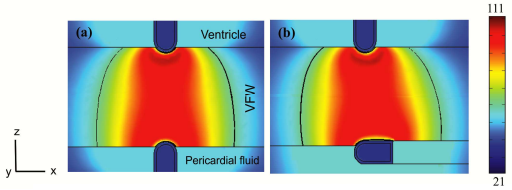

Figure 6. Temperature distributions in tissue after 120 s of bipolar RFA across the VFW (10 mm thickness). Two positions of epicardial catheter examined: placed (a) perpendicular and (b) parallel to the surface.

b) Sequential unipolar mode (SUM): The results of SUM ablation differed significantly from those of BM. Figure 7 shows the temperature distributions in the tissue after RFA for two wall thicknesses, 7.5 and 10 mm, and also for two conditions: air and pericardial fluid around the epicardial electrode.

For ≥10 mm wall thickness, lesions in general took the shape shown in Figure 7c-d, i.e. they were never transmural, either in air or in the pericardial fluid present in the epicardial space. The lesions created on each side of the wall had similar shapes, with depths between 3.7 and 4.1

mm and widths from 6.4 to 7.5 mm (the higher values correspond to the lesions on the epicardial side when the catheter tip is surrounded by air, see Fig.7c). The lesion created on the side of the second activated catheter tip was significantly larger when pericardial fluid was considered to be present than with air (Fig. 7d).
For ≤7.5 mm wall thickness, the lesions were transmural with the shape of an hourglass, as shown in Figure 7a-b. In this case, the lesion on the epicardial side was larger when the electrode was covered by pericardial fluid (Fig. 7b).

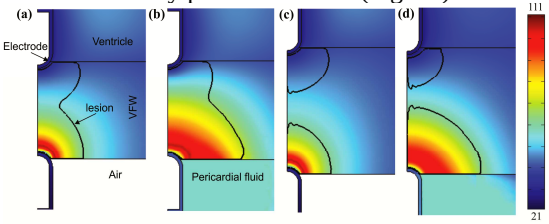

Figure 7. Temperature distributions in tissue after 120 s of sequential unipolar RFA (catheter on top was activated firstly) across the VFW for septal thickness: 7.5 mm with (a) air and (b) pericardial fluid; 10 mm with (c) air and (d) pericardial fluid.

4. Discussion

The objective of the study was to compare sequential unipolar and bipolar RFA across ventricular wall at two sites: 1) the IVS with each electrode located on either side of the septum, and 2) the VFW with one electrode located on the endocardial side of the ventricle and the other on its epicardial surface.

4.1 Interventricular septum (IVS)

The computer modeling results demonstrated that BM created larger lesions than SUM across the IVS. These findings are in agreement with those obtained in previous experimental studies on bipolar ablation of the IVS. Nagashima *et al.*[2] compared both modes using saline-irrigated electrodes on excised swine hearts and found that BM produced a higher number of transmural lesions. Sivagangabalan *et al.*[1] also found that BM required fewer ablations to achieve block across ablation lines and created larger lesions in a post infarct ovine model. Interestingly, we also observed that lesions were not symmetrical during SUM; the lesion was in general larger on the side of the second activated catheter. We believe that this could be due to the result of higher electrical conductivity on the site of the second lesion due to residual heating from the preceding lesion and likely facilitates the deposition of more RF power. The difference in thermal dosage may seem negligible, but our results suggest that this could be significant and may explain the differences in the SUM lesions in previous experimental results[1]. Additionally, we also show that the temperature distributions computed during the bipolar mode when the electrodes are misaligned (Fig. 4. from 2.5 to 10 mm) indicate that transmurality is maintained, which is in agreement with prior experiments[1].

4.2 Ventricular free wall (VFW)

Our results suggest that in the absence of air around the epicardial catheter tip, i.e. when the electrode is completely covered by pericardial fluid, the lesions created across the VFW in BM are transmural. Moreover, the effect on lesion development of the orientation of the catheter tip to the epicardial surface seems to be insignificant (Fig. 6). In contrast, when air is replaced by fluid, BM produces a lesion on the epicardial side only. The simulation of air around the epicardial electrode is relevant, since air could be inadvertently introduced during epicardial puncture. The results of the simulations show that in such a situation, the use of a bipolar RF ablation results in a thermal lesion only on the epicardial side. This is due to the large difference in electrical current density between the catheter tips; the one on the epicardial surface has limited contact with the tissue, resulting in a low effective area and hence a high current density, while the endocardial electrode on the other side is completely covered by cardiac tissue and blood (the electrical conductivity of blood is even higher than cardiac tissue) resulting in a lower current density. As the RF power absorbed by the tissue is directly proportional to the square of current density, lesions will be preferentially created at the epicardial catheter tip due to its high current density as opposed to the endocardial surface.
BM across the VFW when air is present around the epicardial catheter tip should not be considered as a pure bipolar mode, and in fact the temperature distribution shown in Fig. 5a suggests that the electrode on the epicardium actually behaves as the active electrode, whereas the one on the endocardium plays the role of a

dispersive electrode, thus giving negligible heating in its vicinity. SUM is therefore likely to be more effective than BM in achieving transmural lesions (see Fig. 7), at least for smaller wall thicknesses.

4.3 Study Limitations

We only modeled an internally-cooled catheter, since the accurate theoretical modeling of externally irrigated electrodes is somewhat complex at the present time. Although these catheters are used during clinical RF ablation of cardiac tissue,[3] other electrodes such as non and open-irrigated catheters are also employed for cardiac ablation. The conclusions reached in this study could therefore be different when using other catheter designs. In addition, although different lesions could be created when considering: a) different insertion depths of the catheter tip into tissue and b) different voltage/time settings, it is likely that the above conclusions regarding the impact on the lesion geometry of bipolar vs. sequential unipolar ablation, ventricular wall thickness, and misalignment between electrodes will remain essentially unchanged.

5. Conclusions

Our findings suggest that bipolar RFA is superior to sequential unipolar ablation with respect to achieving lesion transmurality within the left ventricle. This holds true for both bipolar IVS and VFW ablation, except in the case of VFW when there is air around the epicardial catheter. Moreover, the orientation of the catheter tip in relation to the epicardial surface during VFW bipolar ablation is irrelevant in terms of lesion shape and depth, and that minor misalignment between the catheter tips during ventricular septal ablation does not interfere with lesion transmurality.

6. References

1. G. Sivagangabalan, MA. Barry et al., Bipolar ablation of the interventricular septum is more efficient at creating a transmural line than sequential unipolar ablation, *Pacing Clin Electrophysiol*, **33**, 16–26 (2012).
2. K. Nagashima, I. Watanabe et al., Lesion formation by ventricular septal ablation with irrigated electrodes: comparison of bipolar and sequential unipolar ablation. *Circ J*, **75**, 565–570 (2011).
3. A. d'Avila, C. Houghtaling et al., Catheter ablation of ventricular epicardial tissue: a comparison of standard and cooled-tip radiofrequency energy, *Circulation*, **109**, 2363-9 (2004).
4. K. Nagashima, I. Watanabe et al., Epicardial ablation with irrigated electrodes: effect of bipolar vs. unipolar ablation on lesion formation, *Circ J*, **76**, 322-7 (2012).
5. E.J. Berjano, Theoretical modeling for radiofrequency ablation: state-of-the-art and challenges for the future, *Biomed Eng OnLine*, **5**, 24 (2006).
6. J.P. Abraham, E.M. Sparrow, A thermal-ablation bioheat model including liquid-to-vapor phase change, pressure- and necrosis-dependent perfusion, and moisture-dependent properties, *Int J Heat Mass Tran*, **50**, 2537-44 (2007).
7. F. Burdío, E.J. Berjano et al., Research and development of a new RF-assisted device for bloodless rapid transection of the liver: Computational modeling and in vivo experiments, *Biomed Eng Online*, **8**, 6 (2009).
8. D. Schutt, E.J. Berjano et al., Effect of electrode thermal conductivity in cardiac radiofrequency catheter ablation: a computational modeling study, *Int J Hyperthermia*, **25**, 99–107 (2009).
9. J.A. Gopalakrishnan, Mathematical model for irrigated epicardial radiofrequency ablation, *Ann Biomed Eng*, **30**, 884–893 (2002).
10. Y. Bilotsky, M. Gasik, Modelling multilayers systems with time-dependent Heaviside and new transition functions, *Proceeding of the Nordic COMSOL Conference* (2006).
11. S.L. Jacques, M.O. Gaeeni, Thermally induced changes in optical properties of heart. *IEEE Eng Med Biol Soc*, 11th Ann Int Conf, **4**, 1199–1200 (1989).

7. Acknowledgements

This work received financial support from the Spanish “Plan Nacional de I+D+I del Ministerio de Ciencia e Innovación” Grant No. TEC2011-27133-C02-01, from Universitat Politècnica de València (PAID-06-11 Ref. 1988). A. González-Suárez is the recipient of a Grant VaLi+D (ACIF/2011/194) from the Generalitat Valenciana.